

# The transition from a TEM-like mode to a plasmonic mode in parallel-plate waveguides

Jingbo Liu, Rajind Mendis,<sup>a)</sup> and Daniel M. Mittleman

*Department of Electrical and Computer Engineering, Rice University, MS-378 6100 Main Street, Houston, Texas 77005, USA*

(Received 25 March 2011; accepted 18 May 2011; published online 10 June 2011)

We describe subwavelength-resolved measurements of the broadband terahertz field propagating inside a finite-width parallel-plate waveguide. We observe a transition in the spatial mode of the waveguide, in which the energy distribution shifts from the waveguide center to the edges with increasing frequency. This transition is surprisingly abrupt, and depends sensitively on the gap between the waveguide plates. These results may have important implications for a variety of terahertz experiments as well as in the design of optical systems and components in the visible and near-infrared regimes, which rely on plasmonic wave guiding. © 2011 American Institute of Physics. [doi:10.1063/1.3598404]

Waveguides with subwavelength cross-sectional dimensions are an important component of many optical systems. In particular, the slot waveguide, two metal plates separated by a small gap, has been studied extensively as a candidate for subwavelength confinement and low-loss guiding.<sup>1,2</sup> Plasmonic modes of this type of waveguide structure can be excited efficiently and propagate for relatively long distances. The slot waveguide is, obviously, structurally homologous to a finite-width parallel-plate waveguide (PPWG). The fundamental TEM mode of the PPWG has a uniform field distribution along the direction perpendicular to the metal surfaces, and is generally considered to be a good description of the spatial mode for many experiments in the terahertz (THz) range.<sup>3–8</sup> This mode is, however, quite distinct from the fundamental plasmonic mode of a slot waveguide, even in the case of very wide metal plates. Here, we show that this distinction is not merely due to the difference in the electromagnetic properties of metals in different frequency regimes but is also intimately related to the geometrical parameters of the PPWG. Using broadband THz time-domain spectroscopy, we observe a rapid transition of the spatial mode with increasing frequency, from the TEM-like mode of a PPWG to the plasmonic mode of a slot waveguide, in a spectral range where the metal's dielectric properties are essentially frequency-independent. We find that the mode transition is surprisingly abrupt, and can be shifted to higher or lower frequency simply by changing the plate spacing. A geometrically induced mode transition of this type has been discussed over 40 years ago<sup>9–11</sup> but has never been studied experimentally.

In the THz regime, metals are good but not perfect conductors, intermediate between the almost ideal metal (infinite conductivity) at microwave frequencies and the much lower conductivity at optical frequencies, which gives rise to strongly bound surface plasmons. In this intermediate regime, the plasmon decay length  $\delta$  above a flat metal surface is typically a few wavelengths for real metal structures.<sup>12–14</sup> As a result, the fundamental mode of a finite-width PPWG depends upon the interplay of three characteristic lengths of comparable magnitude:  $\delta$ , the free-space wavelength  $\lambda$ , and

the distance between the metal plates  $b$ . This interplay results in a complex mode behavior, which is readily observable in the THz regime as presented here.

Our experimental approach is based on scattering probe imaging,<sup>15,16</sup> a technique for characterizing the spatial distribution of a THz field with subwavelength resolution. The concept is similar to apertureless near-field scanning optical microscopy (ANSOM).<sup>17</sup> We mount a subwavelength-sized metal scatterer, typically a short length of thin metal wire, at the end of a dielectric holder. The holder is nearly invisible to THz radiation but the metal object can scatter an incident THz wave toward a receiver. As in ANSOM, the position of the scatterer is modulated using a piezoelectric actuator, so that the signal reaching the detector from the scatterer can be extracted via lock-in detection. Unlike in conventional ANSOM, the detection is phase-sensitive, which has significant advantages.<sup>18</sup> For example, even if the field to be measured is spatially uniform, the differential detection still generates a nonzero signal due to the phase difference induced by modulation of the position of the scatterer relative to the (fixed) THz detector.<sup>15</sup>

We use fiber-coupled photoconductive antennas to generate and detect broadband THz pulses. The waveguide consists of two highly polished aluminum plates having a width of 1 cm and a length of 25 cm, assembled with a variable plate separation  $b$ . The THz beam incident on the input face of the waveguide is polarized perpendicular to the inner plate surfaces to excite the TEM-like mode, and weakly focused to a spot size of  $\sim 1$  cm. The guided wave propagates along the waveguide until it encounters the scattering probe at a distance of 22.5 cm downstream of the input facet. The scattering probe is positioned between the two metal plates, equidistant from both. It oscillates at a frequency of 180 Hz with an amplitude of  $\sim 1$   $\mu\text{m}$ , and can be translated into and out of the PPWG, along a line perpendicular to the waveguide axis.

Figure 1 shows typical waveforms detected at three different locations. The upper-right inset illustrates a cross-section of the PPWG with dots indicating the measurement locations. The lower-right inset shows the corresponding Fourier-transformed spectra, which can be used to characterize the frequency-dependent spatial field distribution. Since

<sup>a)</sup>Electronic mail: rajind@rice.edu.

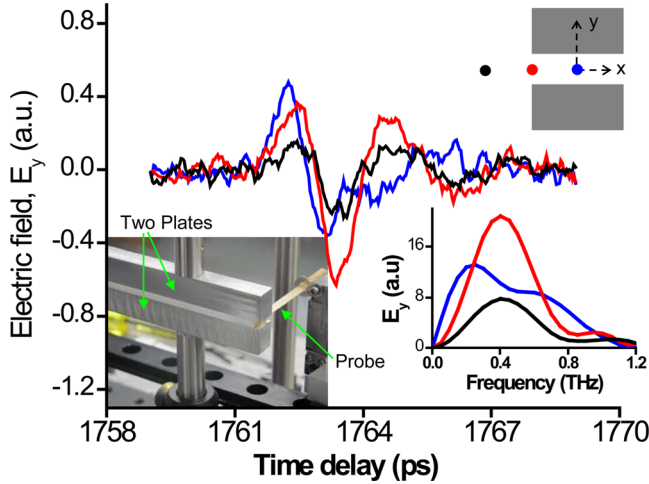


FIG. 1. (Color online) Signals measured inside (blue), at the edge (red), and outside (black) of the waveguide. These locations are illustrated by the cross-sectional view in the upper-right inset. The lower-right inset shows the corresponding spectra, which all have spectral bandwidths similar to that of the input THz pulse. These indicate that the scattering probe technique does not introduce any significant spectral distortion or bandwidth limitation on the measured signals. The left inset shows a photograph of the PPWG with the scattering probe inserted between the plates. The plate-width along the  $x$  direction is 10 mm.

the PPWG is symmetric with respect to the axial plane perpendicular to the plate surfaces, we only need to scan the probe through one half of a transverse plane to map the full distribution. We plot the spectra for each measurement position, and normalize these plots to unity for each frequency, to emphasize the evolution of the spatial distribution of the field with frequency. This result is presented along with its mirror image for clarity in Fig. 2(a), which shows the result for three different plate separations.

We observe a dramatic evolution in the field distribution with increasing frequency, which depends strongly on the plate separation. At low frequencies, the energy is concen-

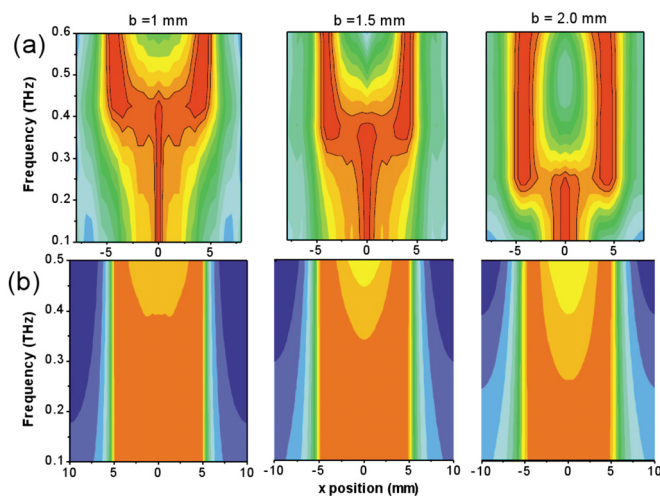


FIG. 2. (Color online) Contour plots of the normalized cross-sectional electric field distribution based on (a) experimental data and (b) numerical simulations using the finite element method. The horizontal axis gives the location of the measurement and the vertical axis gives the frequency. The waveguide extends from  $x = -5$  to 5 mm. Each row of these figures has been normalized to unity, in order to remove the spectral dependence of the input pulse and emphasize the frequency-dependent mode transition. Results for three different values of the plate separation  $b$  are shown.

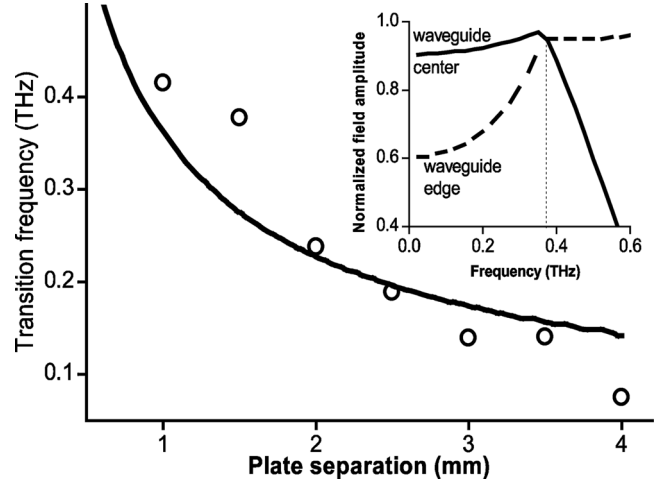


FIG. 3. The transition frequency as a function of the plate separation  $b$ . The black circles are the experimental results and the solid line is the calculated curve from the theoretical model described in the text. The inset shows two vertical cuts extracted from the data of Fig. 2(a), for  $b = 1.5$  mm. The cross-over point of these two curves defines the transition frequency.

trated in the center of the waveguide ( $x=0$ ), as one would expect for the TEM mode.<sup>19</sup> However, at higher frequencies, there is a sharp transition to a different mode, where the energy is concentrated near the waveguide's edges at  $x = \pm 5$  mm. This high-frequency field distribution is strongly reminiscent of the mode of a slot waveguide exhibiting edge plasmons, which has been predicted for optical frequencies<sup>1</sup> and observed in the infrared<sup>20</sup> and THz (Ref. 16) using near-field measurements. All three panels in Fig. 2(a) show qualitatively similar behavior, except that the frequency at which the transition occurs changes with  $b$ . This indicates that the transition from a TEM-like mode to a plasmon-like mode is determined by geometrical parameters, e.g., the dimensionless ratio  $b/\delta$  or  $b/\lambda$ . Evidently, at a particular wavelength one can observe either mode (or any intermediate hybrid<sup>9-11</sup>) simply by varying  $b$ . Figure 2(b) shows numerical two-dimensional simulations of the experimental configuration, based on the finite element method.<sup>21</sup> These simulations do not account for diffractive losses at the waveguide edges, an effect which is larger for lower frequencies. Thus, the low-frequency centralized mode does not weaken at the edges of the PPWG, as it does in the experiments. Nevertheless, the mode transition is accurately reproduced, as well as its sensitivity to  $b$ .

We can further analyze the results of Fig. 2(a) to understand the mechanism responsible for the spatial mode transition. From these results, we extract a characteristic frequency at which the transition from the TEM-like mode to the plasmon-like mode occurs. We plot two vertical slices, at the waveguide center ( $x=0$ ) and edge ( $x=5$  mm), and define the transition frequency as the cross-over point of these two spectral curves. A typical pair of such curves, for  $b = 1.5$  mm, is shown in the inset of Fig. 3, which plots the transition frequencies determined in this manner for various values of  $b$  (circles).

We can interpret the approximate inverse relationship between the transition frequency and  $b$  via an intuitive argument based on surface waves. When  $b$  is much smaller than the decay length  $\delta$ , there is strong coupling between the surface waves propagating on the two plates. Thus, the field

amplitude is nearly constant along a line from one plate to the other, and the mode is similar to the conventional uniform TEM mode.<sup>1,22</sup> However, when  $b$  is comparable to or larger than  $\delta$ , then the mode begins to more closely resemble two-independent surface waves, one on each metal surface, analogous to the hybrid mode described by Barlow.<sup>9–11</sup> For finite-width PPWGs, this field distribution also shows strong enhancements at the edges due to the excitation of edge modes.<sup>1,16</sup> Therefore, the degree of interaction between the two surface waves strongly influences the transition frequency.

We can develop a simple theoretical model to compute this transition frequency and compare to our experimental results. We use the analytical expressions for the TM-polarized waves between two metal plates of infinite width,<sup>22</sup> and model the metal using Drude theory.<sup>23</sup> From these expressions, we can numerically compute the value of the electric field  $E(y)$ , along the  $y$  axis (perpendicular to the plate surfaces). For any chosen value of  $\lambda$  and  $b$ , we can then compute the fractional difference  $\Delta$  between the electric fields at the plate surface and half-way between the surfaces as  $\Delta=[E(0)-E(b/2)]/E(0)$ . For an ideal TEM mode,  $\Delta=0$ ; for two noninteracting surface waves,  $\Delta=1$ . Selecting an arbitrary criterion of  $\Delta=0.05$  as the signature of departure from the low-frequency behavior, we can calculate the transition frequency as a function of  $b$ . The prediction of this model, plotted as a solid line in Fig. 3, agrees reasonably well with the transition frequencies extracted from the experimental data.

In summary, we have conducted frequency-resolved measurements of the spatial mode pattern of a propagating wave inside a finite-width PPWG. We observe a surprisingly abrupt transition in the guided mode, from a TEM-like mode (with energy concentrated in the center of the waveguide) to a plasmon-like mode (with energy concentrated at the

edges). The frequency of the mode transition depends on the geometry of the PPWG, i.e., the plate separation. This is likely to be a general result for many types of plasmonic waveguides, and indicates that the behavior of guided plasmon waves can be influenced as much by geometrical effects as by the dielectric properties of the metal components.

- <sup>1</sup>G. Veronis and S. Fan, *J. Lightwave Technol.* **25**, 2511 (2007).
- <sup>2</sup>D. F. P. Pile, T. Ogawa, D. K. Gramotnev, Y. Matsuzaki, K. C. Vernon, K. Yamaguchi, T. Okamoto, M. Haraguchi, and M. Fukui, *Appl. Phys. Lett.* **87**, 261114 (2005).
- <sup>3</sup>R. Mendis and D. Grischkowsky, *Opt. Lett.* **26**, 846 (2001).
- <sup>4</sup>J. Zhang and D. Grischkowsky, *Opt. Lett.* **29**, 1617 (2004).
- <sup>5</sup>H. Cao, R. A. Linke, and A. Nahata, *Opt. Lett.* **29**, 1751 (2004).
- <sup>6</sup>M. M. Awad and R. A. Cheville, *Appl. Phys. Lett.* **86**, 221107 (2005).
- <sup>7</sup>J. S. Melinger, N. Laman, S. S. Harsha, S. Cheng, and D. Grischkowsky, *J. Phys. Chem. A* **111**, 10977 (2007).
- <sup>8</sup>D. G. Cooke and P. U. Jepsen, *Opt. Express* **16**, 15123 (2008).
- <sup>9</sup>H. E. M. Barlow, *Proc. IEE* **112**, 477 (1965).
- <sup>10</sup>H. E. M. Barlow, *Proc. IEE* **114**, 421 (1967).
- <sup>11</sup>H. E. M. Barlow, *J. Phys. D: Appl. Phys.* **6**, 929 (1973).
- <sup>12</sup>J. Saxler, J. Gómez Rivas, C. Janke, H. P. M. Pellemans, P. Haring Bolívar, and H. Kurz, *Phys. Rev. B* **69**, 155427 (2004).
- <sup>13</sup>T.-I. Jeon and D. Grischkowsky, *Appl. Phys. Lett.* **88**, 061113 (2006).
- <sup>14</sup>L. S. Mukina, M. M. Nazarov, and A. P. Shkurinov, *Surf. Sci.* **600**, 4771 (2006).
- <sup>15</sup>V. Astley, H. Zhan, R. Mendis, and D. M. Mittleman, *J. Appl. Phys.* **105**, 113117 (2009).
- <sup>16</sup>H. Zhan, R. Mendis, and D. M. Mittleman, *Opt. Express* **18**, 9643 (2010).
- <sup>17</sup>B. Knoll and F. Keilmann, *Nature (London)* **399**, 134 (1999).
- <sup>18</sup>K. Wang, D. M. Mittleman, P. C. M. Planken, and N. C. J. Van der Valk, *Appl. Phys. Lett.* **85**, 2715 (2004).
- <sup>19</sup>T. Rozzi and M. Mongiardo, *Open Electromagnetic Waveguides* (IEE, London, 1997).
- <sup>20</sup>R. Yang, M. A. G. Abushaqur, and Z. Lu, *Opt. Express* **16**, 20142 (2008).
- <sup>21</sup>J. Deibel, M. Escarra, N. Berndsen, K. Wang, and D. M. Mittleman, *Proc. IEEE* **95**, 1624 (2007).
- <sup>22</sup>B. G. Ghamsari and A. H. Majedi, *J. Appl. Phys.* **104**, 083108 (2008).
- <sup>23</sup>M. A. Ordal, L. L. Long, R. J. Bell, S. E. Bell, R. R. Bell, R. W. Alexander, and C. A. Ward, *Appl. Opt.* **22**, 1099 (1983).